THE ASTROPHYSICAL JOURNAL, 469:921–935, 1996 October 1

SOLAR WIND FLOW WITH HYDROGEN PICKUP

ILDAR K. KHABIBRAKHMANOV AND DANNY SUMMERS
Department of Mathematics and Statistics, Memorial University of Newfoundland, St. John's, NF, Canada A1C 5S7
AND
GARY P. ZANK AND H. LOUIS PAULS
Bartol Research Institute, University of Delaware, Newark, DE 19716
Received 1995 May 30; accepted 1996 April 16

ABSTRACT

The interaction of the solar wind with neutral interstellar hydrogen is reconsidered. A detailed derivation of the well-known one-fluid hydrodynamic description of the solar wind modified by interstellar pickup ions is presented, based on a semikinetic guiding center description. This analysis clarifies several of the underlying assumptions implicit in Holzer's (1972) model. A brief discussion of stationary solar wind solutions modified by the interstellar neutral gas is given, and, on the basis of this analysis, we deduce that the termination shock may be interpreted as a surface of strong discontinuity with an attached weak discontinuity. Our principal result addresses the stability of the supersonic solar wind in the presence of mass, momentum, and energy loading. It is found that beyond 25 AU a gradient catastrophe can develop, which leads to the formation of the termination shock in the outer heliosphere. The location of the termination shock may be interpreted as due primarily to the properties of the interstellar neutrals (such as the value of their number density) rather than as due entirely to the balancing of the solar wind dynamic pressure and interstellar plasma pressure. Examples of recent multidimensional computations of the interaction of the solar wind with the local interstellar medium that include interstellar neutrals in a fully self-consistent manner are presented, and these provide support for the simpler one-dimensional analysis.

Subject headings: hydrodynamics — ISM: general — shock waves — solar wind

1. INTRODUCTION

The free expansion of the solar wind beyond the sonic point in Parker's (1958) original model is unrestricted. The solar wind speed u is almost constant for $r > 10$ AU, and the density ρ decays roughly as r^{-2}; the Mach number of the solar wind $M = \rho u^2/\gamma P$ (where γ is the specific heat ratio and P the plasma pressure) grows without bound. In this picture, the collision of the solar wind with the interstellar medium would result in a very strong shock (see, e.g., the review of gasdynamic interaction models by Baranov 1990). However, it became clear subsequently that the neutral hydrogen component of the local interstellar medium (LISM), which is quite dense (at least 0.1 cm^{-3}) and is moving relative to the Sun with velocity $V_\infty \approx 26$ km s^{-1}, should restrict the expansion of the solar wind. Although the densities are too low for the direct interaction of the solar wind plasma flow with the neutral flux, the solar wind plasma is magnetized, and appreciable momentum and energy exchange is possible via charge exchange between solar wind protons and neutral hydrogen. In a plasma with a sufficiently strong magnetic field, a newly charged particle will gain a gyrospeed equal to its initial velocity relative to the plasma and will start to move with the plasma flow during the time of one gyroperiod. The microscopic aspects of this process may be rather complicated. For example, the velocity distribution function of newly produced, charged particles might be unstable, which would cause further modification of the bulk interaction. The net result of the process on hydrodynamic scales is, however, qualitatively unique: there is a change in the density, momentum, and energy of the plasma flow for each act of charged particle production (or destruction). The basic model was formulated by Wallis (1971) and Holzer (1972). Holzer (1972) gave an extensive analysis which, like Wallis (1971), included the possibility of a shock-free interaction of the solar wind with the LISM. The purpose of this investigation is to explore the underlying assumptions implicit in the model, to simplify it as far as possible in the supersonic region without losing essential features, and to study the stability properties of the loaded solar wind flow.

The detailed investigation of pickup processes in the solar wind was given great impetus recently by spacecraft observations of the interaction of a cometary coma with the solar wind (e.g., Galeev 1991). As a result, we possess now a reasonable understanding of pickup processes at different spatial and timescales ranging from hydrodynamic to microscopic structures, and from long to short timescale evolution. It has been recognized that the pickup process and subsequent evolution of the pickup ion distribution determines many of the structural features in the cometary environment. The solar wind begins to decelerate at large distances from the cometary nucleus, at which the ionization of a very small number of neutral molecules produces relatively important changes in the solar wind momentum. The distance to the cometary bow shock is determined by the neutral gas outflow rate, as is the location of the contact discontinuity. As for the pickup of interstellar hydrogen by the solar wind, it is obvious that the solar wind should be decelerated. What is not clear, however, is whether the solar wind–LISM interaction is strong enough to determine the basic characteristics of the solar wind flow in the distant heliosphere (as is the analogous case for comets), or whether it produces merely a minor modification to an essentially thermal solar wind; see the review by Holzer (1989). In terms of the solar wind Mach number M, if the pickup process can decrease the Mach number so that $M \approx 1$, then pickup is important, and we should expect new features in the solar wind that reflect the character of the pickup process. If, on the other hand, the Mach number remains large ($M \gg 1$) everywhere, we can largely

ignore its influence on the solar wind.

In § 2, we present a simple semikinetic model that is motivated largely by recent cometary research, and we explore the underpinnings of the Holzer (1972) basic model. Some limiting cases are analyzed in detail in § 3, and the stability properties of the stationary flow are examined in § 4.

2. SEMIKINETIC MODEL FOR HYDROGEN PICKUP BY THE SOLAR WIND

Under the assumption that the plasma particles are magnetized, we shall use the guiding center kinetic equation for the particle distribution function $f(\boldsymbol{r}, \mu, v_{\parallel}, t)$ (e.g., see Kulsrud 1983 and Khabibrakhmanov, Galinsky, & Verheest 1992):

$$\frac{\partial f}{\partial t} + \nabla \cdot [(\boldsymbol{U} + v_{\parallel}\boldsymbol{b})f] + \frac{\partial}{\partial v_{\parallel}}\left[\boldsymbol{b}\cdot\nabla\left(-\frac{q_i\varphi}{m_e} - \mu B + \frac{U^2}{2}\right) + \boldsymbol{b}\cdot\boldsymbol{g} - v_{\parallel}\,\boldsymbol{b}\cdot\nabla\boldsymbol{U}\cdot\boldsymbol{b}\right] f = \mathrm{St}\,\{f\}\,, \tag{1}$$

where $\mu = v_{\perp}^2/2B$ is the particle magnetic moment; $v_{\parallel}$ and $v_{\perp}$ are components of the particle velocity parallel and transverse to the direction of the local magnetic field $\boldsymbol{B}$, which has the unit direction vector $\boldsymbol{b} = \boldsymbol{B}/B$; $\boldsymbol{U}$ is the bulk flow velocity of the solar wind, which is essentially the drift velocity in the electromagnetic field $\boldsymbol{U} = c(\boldsymbol{E}\times\boldsymbol{B})/B^2$; φ is the potential of the electric field along the magnetic field lines, so that $\boldsymbol{b}\cdot\nabla\varphi + \boldsymbol{b}\cdot\boldsymbol{E} = 0$; q_i is the electric charge of the plasma particle; $\boldsymbol{g} = -\boldsymbol{r}GM_{\odot}/r^3$ is the gravitational acceleration; and $\boldsymbol{r}$ is the position vector. Note that the expression for the drift velocity $\boldsymbol{U}$ is general in the sense that it contains the turbulent magnetohydrodynamic (MHD) wave electromagnetic field. We include on the left-hand side only the response of the particle to adiabatic changes of the large-scale magnetic field. Thus, the left-hand side conserves the magnetic moment of an individual particle; there is no differentiation with respect to μ. All other interactions are collected into the "collision" term on the right-hand side, St. The term denotes Coulomb collisions in the case of a quiet plasma, or the interaction of plasma waves with ions in a turbulent plasma far from thermal equilibrium; in this paper we assume that Coulomb collisions can be ignored. Most important for a pickup process, St can denote also the source and sink terms for the plasma particles. It is clear how the source and sink of the plasma particles appear at the microlevel. These terms are proportional to the rate $\hat{v}[F(\boldsymbol{v}), f(\boldsymbol{v})]$ of supply or destruction of particles with a given velocity $\boldsymbol{v}$; $\hat{v}$ is in general a complicated functional of the distribution functions of both plasma particles $f(\boldsymbol{v})$ and neutral particles $F(\boldsymbol{v})$.

For photoionization, which has been studied extensively at comets, one has the relatively simple source term,

$$\nu_{\mathrm{ph}}(r)F(\boldsymbol{v})\,, \tag{2}$$

where the rate of photoionization ν_{ph} is defined completely by the UV photon flux from the Sun and depends only on the distance from the Sun, i.e., $\nu_{\mathrm{ph}} \propto r^{-2}$. A more complicated dependence on distance can appear if there is an appreciable extinction of the photon flux.

The case of charge exchange is more complex. As a result of the charge exchange of a proton with velocity $\boldsymbol{v}'$ and a hydrogen atom with velocity $\boldsymbol{v}$, we obtain a hydrogen atom with velocity $\boldsymbol{v}'$ and a proton with velocity $\boldsymbol{v}$. The probability of this reaction occurring is determined by the corresponding cross section $\sigma_c(|\boldsymbol{v}-\boldsymbol{v}'|)$, and the collision term corresponding to the charge exchange reaction takes the rather complicated general form (Holzer & Banks 1969)

$$\int d^3\boldsymbol{v}'\,|\boldsymbol{v}-\boldsymbol{v}'|\sigma_c(|\boldsymbol{v}-\boldsymbol{v}'|)[F(\boldsymbol{v})f(\boldsymbol{v}') - F(\boldsymbol{v}')f(\boldsymbol{v})]\,. \tag{3}$$

Some assumptions will be made at this stage to allow an analytical treatment. For instance, we assume that the neutral velocity is small compared to the proton velocity. Such is the case for the solar wind since the neutral velocity is now measured to be about 26 km s^{-1}, with a small thermal spread (Lallement, Bertaux, & Clarke 1993). The source term can then be expressed as

$$F(\boldsymbol{v})\int d^3\boldsymbol{v}'\,|\boldsymbol{v}'|\sigma_c(|\boldsymbol{v}'|)f(\boldsymbol{v}') = F(\boldsymbol{v})\langle\sigma_c\, v\rangle\,. \tag{4}$$

Here $\langle\sigma_c\, v\rangle$ is the rate of production of new hot neutral particles with a distribution function $F(\boldsymbol{v})$ as a result of charge exchange. The sink term can be expressed as

$$f(\boldsymbol{v})|\boldsymbol{v}|\sigma_c(|\boldsymbol{v}|)\int d^3\boldsymbol{v}'\,F(\boldsymbol{v}') = f(\boldsymbol{v})\sigma_c(v)vN\,. \tag{5}$$

The particle velocity $\boldsymbol{v}$ in the laboratory frame of reference (which appears on the right-hand side of eq. [1]) and the guiding center variables $(v_{\perp}, v_{\parallel}, \phi)$ are related through the results $v_{\parallel} = \boldsymbol{v}\cdot\boldsymbol{b}$ and $v_{\perp} = |(\boldsymbol{v}-\boldsymbol{U})\times\boldsymbol{b}|$. By using this transformation, the right-hand side of equation (1) can be expressed in terms of the guiding center variables alone, and the gyrophase average can be performed explicitly.

The particle density is defined by the zeroth moment of equation (1), which gives the continuity of particle mass density, namely,

$$\frac{\partial\rho}{\partial t} + \nabla\cdot\boldsymbol{u}\rho = \nu_{\mathrm{ph}}Nm\,, \tag{6}$$

where

$$\boldsymbol{u} = \boldsymbol{U} + \boldsymbol{b}U_{\parallel}, \qquad U_{\parallel} = \frac{\int d^3\boldsymbol{v}\, v_{\parallel} f(\boldsymbol{v})}{\int d^3\boldsymbol{v} f(\boldsymbol{v})} .$$

For the bulk velocity $\boldsymbol{u}$ of the plasma, taking the first moment of equation (1) yields the momentum equation in the form

$$\frac{\partial \boldsymbol{u}}{\partial t} + \boldsymbol{u}\cdot\nabla\boldsymbol{u} + \nabla P = -\nu_{\rm ph} Nm \frac{\boldsymbol{u}}{\rho} - \langle\sigma_c v\rangle N\boldsymbol{u} . \tag{7}$$

Although the magnetic field might be omitted completely at the hydrodynamic level, when the magnetic pressure is small compared to the thermal pressure P and kinematic pressure ρu^2 of the gas, the geometry of the pickup ion interaction and its physical properties are defined by the angle between the magnetic field direction and flow direction. If the magnetic field is orthogonal to both the plasma flow and neutral particle flow, then newly born ions acquire motion only in the plane orthogonal to the magnetic field direction, and $v_{\parallel} = 0$. Thus, newly born particles have 2 degrees of freedom, implying that the particles behave on hydrodynamic scales as a gas with specific heat ratio $\gamma = 2$. If we ignore completely the motion of ions parallel to the magnetic field direction in equation (1), then the kinetic equation for the distribution function is

$$\frac{\partial f(u,\mu)}{\partial t} + \nabla\cdot[\boldsymbol{u}f(u,\mu)] = \nu_{\rm ph} mN\delta\left(\mu - \frac{mu^2}{2B}\right) + \langle\sigma_c v\rangle Nm\left[\delta\left(\mu - \frac{mu^2}{2B}\right) - f(u,\mu)\right], \tag{8}$$

where we have assumed that the neutral particle velocity distribution is a delta function (at rest in the laboratory frame of reference),

$$F(\boldsymbol{v}) = N\delta(\boldsymbol{V}) .$$

More realistic, however, is the case in which the magnetic field is not orthogonal to the direction of the neutral flux. In this case, we have an additional degree of freedom, and most important, there is bulk motion of the newly born particles relative to the rest of the plasma. The situation is unstable, with the pickup ions exciting parallel-propagating Alfvén waves that induce almost elastic scattering of the ions. The scattering is rapid on the timescales of the gyroperiod of the plasma particles and leads to an almost complete isotropization of the pickup ion distribution. The particles then behave as a perfect gas with $\gamma = 5/3$. Formally, this result can be obtained from equation (1) if we take into account strong elastic scattering of the plasma particles by MHD turbulence. It is convenient to rewrite equation (1) using spherical coordinates in velocity space, with the polar axis along the radial direction outward from the Sun ($v_{\parallel} = U_{\parallel} + v\cos\theta_v = U_{\parallel} + v\xi$ and $v_{\perp} = v\sin\theta_v$). If $U_{\parallel}$ is the bulk velocity of the plasma along the magnetic field, we have

$$\frac{\partial f}{\partial t} + \nabla\cdot[(\boldsymbol{U} + U_{\parallel}\boldsymbol{b} + v\xi\boldsymbol{b})f] + \left(\xi\frac{\partial}{\partial v} + \frac{1-\xi^2}{v}\frac{\partial}{\partial\xi}\right)\left[\boldsymbol{b}\cdot\nabla\Phi - \frac{v^2(1-\xi^2)}{2}\boldsymbol{b}\cdot\nabla\ln B - (U_{\parallel} + v\xi)U\boldsymbol{b}\cdot\nabla\boldsymbol{n}\cdot\boldsymbol{b}\right]f = \mathrm{St}\,\{f\} , \tag{9}$$

where $\Phi = e\varphi/m + U^2/2 - \varphi_g$ is a generalized potential, with the gravitational potential $\varphi_g = -GM_{\odot}/r$ defined so that $\boldsymbol{g} = -\nabla\varphi_g$. It is assumed that the background magnetic field is in the radial direction. Unit vectors are $\boldsymbol{n} = \boldsymbol{U}/U$ and $\boldsymbol{b} = \boldsymbol{B}/B$, and it is assumed that the Alfvén waves have the property that the vectors $\boldsymbol{b}$, $\boldsymbol{n}$, and the propagation direction vector $\boldsymbol{r}$ lie in one plane.

Equation (9) can be written in the equivalent conservation form

$$\nabla\cdot[(\boldsymbol{U} + U_{\parallel}\boldsymbol{b} + v\xi\boldsymbol{b})f] - \frac{1}{v^2}\frac{\partial}{\partial v}v^2\left[\frac{v}{3}U\boldsymbol{b}\cdot\nabla\boldsymbol{n}\cdot\boldsymbol{b}f + A(v,\xi,r)(1-\xi^2)\frac{\partial f}{\partial\xi}\right] + \frac{\partial}{\partial\xi}A(v,\xi,r)(1-\xi^2)\frac{\partial f}{\partial v} = \mathrm{St}\,\{f\} , \tag{10}$$

where

$$A(v,\xi,r) = \frac{v\xi}{3}U\boldsymbol{b}\cdot\nabla\boldsymbol{n}\cdot\boldsymbol{b} - \frac{1}{2}(\boldsymbol{b}\cdot\nabla\Phi - U_{\parallel}U\boldsymbol{b}\cdot\nabla\boldsymbol{n}\cdot\boldsymbol{b}) + \frac{v^2(1-\xi^2)}{8}\boldsymbol{b}\cdot\nabla\ln B . \tag{11}$$

The assumption of strong scattering allows us to average equation (10) over θ to obtain an equation for the isotropic part of the distribution function (see, for example, Galeev 1991). The equation is

$$\frac{\partial f}{\partial t} + \nabla\cdot\boldsymbol{u}f - \frac{1}{3v^2}\frac{\partial}{\partial v}(v^3 f\nabla\cdot\boldsymbol{u}) = \frac{\nu_{\rm ph}}{v^2}\delta(u-v) - \sigma_c vNf + \frac{N}{v^2}\delta(u-v)\langle\sigma_c v\rangle , \tag{12}$$

where, for simplicity, we have neglected the terms involving the magnetic field and gravity. The limiting forms (8) and (12) of the kinetic equation (1) are very different, as are the solutions for the plasma particle distribution function. The situation is changed significantly if, instead of solving equations (8) or (12), we describe the plasma flow by means of the second moment of the distribution function, i.e., the particle pressure. In both limiting cases, we have a single equation for the particle pressure in which the appropriate values for the specific heat ratio (2 or 5/3) must be substituted.

Accordingly, the model to be investigated consists of the three equations,

$$\rho_t + \frac{1}{r^2}(r^2 un)_r = \nu_{\rm ph} N\,, \tag{13}$$

$$\rho u_t + \rho u u_r + P_r = -\nu_{\rm ph} mNu - \langle \sigma_c v\rangle N\rho u\,, \tag{14}$$

$$P_t + uP_r + \gamma P u_r + \frac{2}{r}\gamma P u = (\gamma - 1)\nu_{\rm ph} mN\frac{u^2}{2} - \langle \sigma_c v\rangle N\left[P - (\gamma - 1)\rho\frac{u^2}{2}\right]. \tag{15}$$

As noted above, $\gamma = 2$ for quasi-perpendicular interactions, while $\gamma = 5/3$ for oblique and parallel geometries.

The neutral gas density, in general, has to be found self-consistently. For a given neutral gas flux $N_\infty V_\infty$ at infinity, the neutral gas number density along the stagnation line is obtained from the corresponding neutral gas continuity equation,

$$-\frac{d(VN)}{dr} = -\nu_{\rm ph} N - \langle \sigma_c v\rangle Nn\,. \tag{16}$$

It is important to note that equation (16) is not only an additional differential equation to be solved, but the equation turns the problem into a boundary value problem. This is because we specify the neutral gas density at large r, whereas all the solar wind parameters are given at some distance close to the Sun (typically 1 AU).

Again, we can simplify the situation considerably if, in calculating $\langle \sigma_c v\rangle$, we restrict our attention to supersonic plasma flow and neglect the thermal motion of the plasma particles. A more extensive hydrodynamic description that does not make this assumption has been developed by Pauls, Zank, & Williams (1995). Assuming that the charge exchange cross section is velocity independent, we can use the approximation

$$\langle \sigma_c v\rangle = \sigma_c u\,.$$

By means of the dimensionless variables

$$r \to \frac{r}{r_E}\,, \qquad \rho \to \frac{\rho}{\rho_E}\,, \qquad u \to \frac{u}{u_E}\,, \qquad P \to \frac{P}{\rho_E u_E^2}\,, \qquad N \to \frac{N}{N_\infty}\,, \tag{17}$$

we can rewrite our model equations as follows:

$$\frac{1}{N}\frac{dN}{dr} = \kappa\left(\frac{\beta}{r^2} + \alpha nu\right), \tag{18}$$

$$\frac{1}{r^2}(r^2 un)_r = \beta\frac{N}{r^2}\,, \tag{19}$$

$$\rho u u_r + P_r = -\beta u\frac{N}{r^2} - \alpha N\rho u^2\,, \tag{20}$$

$$uP_r + \gamma P u_r + \frac{2}{r}\gamma P u = (\gamma - 1)\beta\frac{N}{r^2}\frac{u^2}{2} - \alpha Nu\left[P - (\gamma - 1)\rho\frac{u^2}{2}\right], \tag{21}$$

where

$$\alpha = \sigma_c N_\infty r_E\,, \qquad \beta = \frac{\nu_{\rm ph}^E N_\infty r_E}{n_E u_E}\,, \qquad \kappa = \frac{n_E u_E}{N_\infty V_\infty}\,.$$

The momentum and energy equations can be transformed into the respective conservation forms,

$$(\rho u)_t + \frac{1}{r^2}(r^2\rho u^2)_r + P_r = -\alpha N\rho u^2\,, \tag{22}$$

$$\left(\frac{\rho u^2}{2} + \frac{1}{\gamma - 1}P\right)_t + \frac{1}{r^2}\left[r^2 u\left(\frac{\rho u^2}{2} + \frac{\gamma}{\gamma - 1}P\right)\right]_r = -\alpha Nu\left(\frac{1}{\gamma - 1}P + \frac{\rho u^2}{2}\right). \tag{23}$$

The right-hand sides of equations (22)–(23) have exactly the same form as that used by Holzer (1972), except for the terms accounting for the magnetic field pressure and the finite thermal velocities of the plasma and neutral hydrogen. For typical solar wind parameters, these effects have quite a small influence on the interaction involving the supersonic solar wind (Holzer 1972), and so we shall ignore them in order to keep the analysis as simple as possible.

3. ANALYTICAL SOLUTIONS

The system of four differential equations (18)–(21) is decoupled, since the neutral gas density and plasma continuity equations include only the neutral gas density N and plasma density flux nu. These two first-order differential equations can

be combined into a single second-order differential equation,

$$\frac{d}{dr}\frac{r^2}{N}\frac{dN}{dr} = \kappa\alpha\beta N , \tag{24}$$

for which we have the boundary conditions

$$N_{r=\infty} = 1 , \qquad \left.\frac{d\ln N}{dr}\right|_{r=1} = \kappa(\beta + \alpha) . \tag{25}$$

After substituting

$$N = \exp\left[-\frac{\kappa(\alpha+\beta)}{r} + y(x)\right], \qquad x = -\frac{1}{r} ,$$

in equation (24), we obtain an equation for $y(x)$ with homogeneous boundary conditions,

$$x^2\frac{d^2y}{dx^2} = \kappa\alpha\beta \exp\left[\kappa(\alpha+\beta)x + y(x)\right] , \qquad y(0) = 0 , \qquad y'(-1) = 0 . \tag{26}$$

A commonly used expression for the neutral gas density profile N with $y(x) = 0$ is the zero-order term in the expansion of equation (24) in terms of the small parameter $\kappa\alpha\beta$, namely,

$$N = \exp\left[-\kappa(\alpha+\beta)/r\right] ,$$

which gives a fairly accurate description for actual heliospheric parameters. We can see from this result that neutral hydrogen penetrates deep into the heliosphere, with a characteristic depth $\kappa(\alpha+\beta) \approx 7.5$ AU, and so it can be observed at the Earth's orbit.

In the present paper, we are considering only the dynamics of the interstellar neutral hydrogen. However, as a result of charge exchange there is also a newly created flow of high-speed solar wind neutral hydrogen. This component will also interact with the interstellar wind with a potential for heating and decelerating the wind, though we do not address such effects here.

The remaining equations for the plasma momentum and energy are transformed to

$$\frac{M^2-1}{2u^2}\frac{du^2}{dr} = \frac{2}{r} - \alpha N\left(\frac{\gamma+1}{2}M^2 - \frac{1}{\gamma}\right) - \frac{\beta N}{r^2\rho u}\frac{\gamma+1}{2}M^2 , \tag{27}$$

$$\frac{(M^2-1)}{c^2}\frac{dc^2}{dr} = -(\gamma-1)\frac{2}{r}M^2 + \alpha N\left(\gamma\frac{\gamma-1}{2}M^4 - \frac{3-\gamma}{2}M^2 + \frac{1}{\gamma}\right) + \frac{\beta N}{r^2\rho u}\left(\gamma\frac{\gamma-1}{2}M^4 - \frac{3-\gamma}{2}M^2 + 1\right), \tag{28}$$

where we have introduced the sound speed $c^2 = \gamma P/\rho$ and Mach number $M = u/c$. Combining equations (27) and (28), we obtain an equation for M^2,

$$\frac{M^2-1}{M^2}\frac{dM^2}{dr} = \frac{2}{r}\left[2 + (\gamma-1)M^2\right] - \alpha N\left[\frac{\gamma(\gamma-1)}{2}M^4 + \frac{3\gamma-1}{2}M^2 - \frac{1}{\gamma}\right] - \frac{\beta N}{r^2\rho u}\left[\frac{\gamma(\gamma-1)}{2}M^4 + \frac{3\gamma-1}{2}M^2 + 1\right]$$

$$= \frac{2}{r}\left[2 + (\gamma-1)M^2\right] + \alpha N\frac{\gamma+1}{\gamma} - \frac{N}{2}\left(\alpha + \frac{\beta}{r^2\rho u}\right)(\gamma M^2 + 1)\left[(\gamma-1)M^2 + 2\right] . \tag{29}$$

3.1. *Free Expansion*

The neglect of all loading effects, i.e., setting $\alpha = 0$ and $\beta = 0$, and retention of only the effects of geometrical expansion, yields solutions to equation (29) in the form

$$\left[2 + (\gamma-1)M^2\right]^{(\gamma+1)/(\gamma-1)} = \text{const } M^2r^4 . \tag{30}$$

Solution (30) represents simple, free, adiabatic expansion of the solar wind with an asymptotic Mach number $M \propto r^{\gamma-1}$.

3.2. *Plane Geometry and No Charge Exchange*

If we set $\alpha = 0$ (corresponding to no charge exchange) and neglect the geometrical effects of spherical expansion in the first term on the right-hand side of equation (29), then we obtain the solution

$$\frac{\rho u(1+\gamma M^2)}{M^2\left[2 + (\gamma-1)M^2\right]} = \text{const} . \tag{31}$$

Solution (31), which corresponds to a plane geometry, has been found in cometary physics, and it follows from the conservation of momentum and energy flux (see eqs. [22]–[23]). The mass flux ρu as a function of distance alone follows readily from the plasma continuity equation, and so result (31) can be used to locate a point in the flow with a given Mach number. In the case of comets, it was found from numerical experiments, and later confirmed by direct observations, that the Mach number of a cometary shock is close to 2 (Galeev 1991). A theoretical stability analysis showed that an instability exists in the mass-loaded flow with $M < 2.9$, and that the nonlinear evolution of the instability takes the form of a gradient catastrophe

with an explosive growth in time. The conclusion was drawn that the Mach number of the mass-loaded solar wind flow near the cometary bow shock is always close to 2. Expression (31) thus provides a means of finding the distance to the shock transition, when mass-loading is due to photoionization exclusively.

3.3. *No Photoionization, Plane Geometry*

At 1 AU, the charge exchange rate is an order of magnitude larger than photoionization. This relationship continues to hold approximately in the outer heliosphere; also, since $\nu_{ph} \propto r^{-2}$, it follows that $nu \propto r^{-2}$ approximately. It is interesting to note that although the cometary community was well aware of this fact (e.g., Galeev 1991), it has been nonetheless ignored, at least at an analytical level, in the interests of simplicity.

If we retain only the second term in equation (29), i.e., the term responsible for charge exchange, we find

$$\int dr\, \alpha N = \frac{\gamma}{2} \ln\left[\frac{(M^2 + b)^{\mu-1}}{(M^2 - a)^{\mu+1}} M^4\right], \tag{32}$$

where

$$\mu = \frac{3\gamma - 4}{\gamma}\sqrt{\frac{\gamma + 1}{9\gamma - 7}}, \qquad a = \frac{\sqrt{(\gamma + 1)(9\gamma - 7)} - 3\gamma + 1}{2\gamma(\gamma - 1)}, \qquad b = \frac{\sqrt{(\gamma + 1)(9\gamma - 7)} + 3\gamma - 1}{2\gamma(\gamma - 1)}.$$

3.4. *General Solutions*

In the general case, a solution in closed form cannot be obtained. It is clear from equation (29) that, in the absence of expansion, continuous flow through the sonic point $M = 1$ is not possible since the right-hand side cannot be zero at $M = 1$; a shock transition must therefore be present. The spherical expansion of the solar wind introduces the possibility for a smooth transition, however. This is analogous to the acceleration of the solar wind through the sonic point in Parker's (1958) solar wind model, but with an important difference. Since the sonic point near the Sun is a saddle point in Parker's model, only one physically meaningful solution passes along a separatrix through the critical point. In the present situation, the topology of the solutions in the vicinity of the critical point is more complicated, as we shall describe below.

A numerical evaluation of the Mach number profiles for the system (18)–(21) is presented for the following solar wind and interstellar medium parameters:

$$\sigma_c = 5 \times 10^{-15}\ \mathrm{cm}^2, \quad n_E u_E = 3 \times 10^8\ \mathrm{cm}^{-2}\ \mathrm{s}^{-1}, \quad N_\infty = 0.1\ \mathrm{cm}^{-3}, \quad V_\infty = 20\ \mathrm{km\ s}^{-1}, \quad \nu_{ph}^E = 9 \times 10^{-8}\ \mathrm{s}^{-1}.$$

Initial Mach numbers of $M = 2$, 4, and 6 for the solar wind at 1 AU are assumed, and the results are plotted in Figure 1. As expected physically (and indeed quantitatively from the equation of free expansion [30]), the Mach number profiles increase with distance to the point $\approx$7.5 AU, at which the neutral hydrogen density becomes substantial. Beyond this point, charge exchange becomes sufficiently effective to decelerate the flow and decrease the Mach number.

A feature of the Mach number profiles is that all three are identical at large distances. This is a consequence of the nature of the singularity of the system at the sonic point. The sonic point is an improper node with two separatrices. All physically meaningful solutions in the upstream region approach the sonic point along the lower separatrix, and the low Mach number

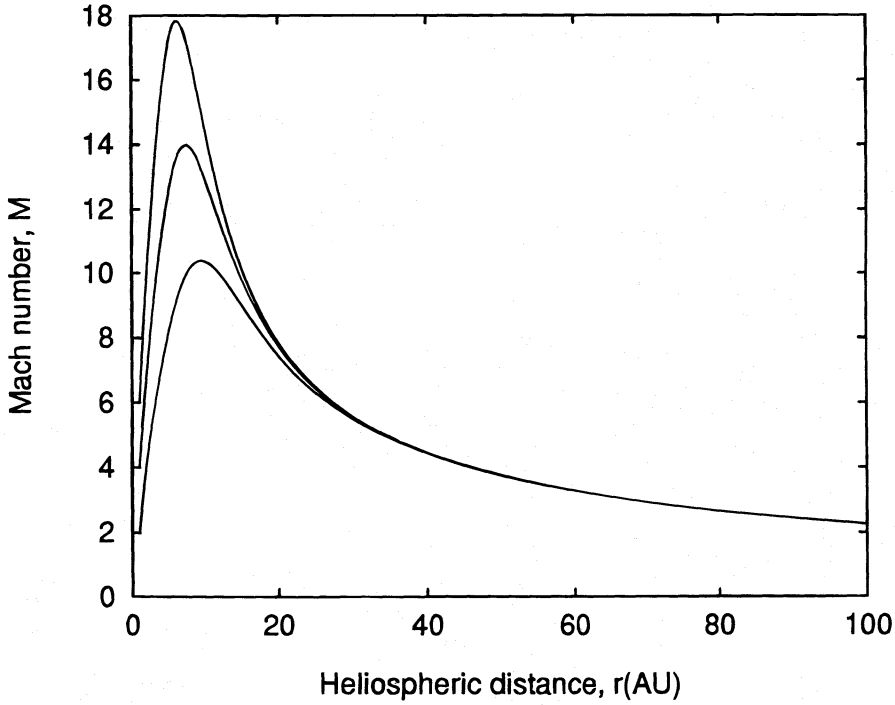

FIG. 1.—Profiles of the Mach number M for the three cases $M = 2$, 4, and 6, at $r = 1$ AU, for the specific heat ratio $\gamma = 5/3$

solutions are indistinguishable from the separatrix. To illustrate the solutions, it is convenient to follow Wallis (1971) and introduce the new dependent variable

$$\eta = \gamma \frac{M^2 - 1}{\gamma M^2 + 1} . \tag{33}$$

Then equation (29) takes the form

$$\eta \frac{d\eta}{dr} = \frac{2}{r} \frac{(\gamma^2 - \eta^2)(1 - \eta)}{\gamma + 1} + \alpha N \frac{(\gamma + \eta)(1 - \eta)^2}{\gamma + 1} - \frac{N}{2} \left(\alpha + \frac{\beta}{r^2 \rho u} \right) (\gamma^2 - \eta^2) . \tag{34}$$

As was pointed out by Wallis (1971) and Holzer (1972), in an expanding solar wind the sonic point of the flow is found by equating the right-hand side of equation (34) to zero, together with $\eta = 0$, i.e.,

$$R_s = \frac{4\gamma}{(\gamma - 1)(\gamma + 2)\alpha + (\gamma + 1)\gamma\beta/(r^2 \rho u)} . \tag{35}$$

Result (35) was obtained in the limit $N \approx 1$, which is valid for $r \gg 1$. Notice that if, as in the case of the solar wind, $\beta \ll \alpha$, then the distance to the sonic point is defined only by the parameter α which in turn is proportional to N_∞, and it does not depend on the flow conditions at small distances (near 1 AU).

Near the sonic point, the solution for η can be expressed as

$$\eta^2 = a\eta(r - R_s) + b \frac{(r - R_s)^2}{2} + \cdots , \tag{36}$$

where

$$a = \left. \frac{d\eta}{dr} \right|_{r = R_s, \eta = 0} = -\frac{\gamma^2}{2} \left(\alpha + \frac{\beta}{r^2 \rho u} \right) - \frac{\gamma - 1}{\gamma + 1} \alpha ,$$

$$b = \eta \left. \frac{d^2\eta}{dr^2} \right|_{r = R_s, \eta = 0} = -\frac{\gamma^2(\gamma + 1)}{8} \left(\alpha + \frac{\beta}{r^2 \rho u} \right)^2 + \frac{\gamma}{2} \left(\alpha + \frac{\beta}{r^2 \rho u} \right) \alpha - \frac{1}{2(\gamma + 1)} \alpha^2 .$$

Expression (36) can be used, as in the cometary case, to find the distance to the point in the solar wind flow with a given critical value of the Mach number M_{cr}.

If we assume that, as in the cometary case, the critical Mach number M_{cr} of the termination shock is defined by the internal stability of the mass-loaded flow, the previous property suggests that the distance to the termination shock is determined only by the neutral gas density N_∞. Such a criterion provides a quite different perspective in specifying the location of the termination shock, for it has been supposed generally that the location is determined by the force balance between the solar wind and interstellar medium. The force-balance argument, of course, is certainly valid if one ignores the loading effects in the subsonic part of the solar wind. Again, if we refer to the case of comets, the subsonic solar wind behavior is determined completely by the effects of mass loading and momentum addition, to the extent that the solar wind flow stagnates completely at a distance defined only by the outgassing rate of neutral molecules.

One important point not discussed by Wallis (1971) and Holzer (1972) in their original analysis is that the double-valued function of equation (36) represents two separatrices at an improper node. Continuous flow is represented by the solution whose tangent to the function $\eta(r)$ is the same on both sides of the sonic point. In principle, it is possible for the solution to choose other separatrices after crossing the sonic point. The flow has continuous velocity, pressure, and density, but it has a finite jump in the first derivatives of all three parameters. This type of discontinuity is known in fluid mechanics as a weak discontinuity (see, e.g., Landau & Lifshitz 1987). A weak discontinuity always propagates along the characteristics, so that its speed of propagation is one of u, $u + c$, $u - c$. The stationary weak discontinuity can thus exist only at the sonic point $u = c$, and the jump conditions for the derivatives are defined by the discontinuity in the tangents for the two different separatrices in equation (36). Such a weak transition may even be physically preferable to a smooth transition, as most physically realistic solutions at large distances are attracted by the second separatrix (Wallis 1971, Fig. 1). In the case in which a smooth solution behaves improperly in the subsonic region, the possibility of a weak discontinuity at the sonic point adds a new solution.

By introducing a small but finite viscosity into the system, we can determine which of the two possibilities can be realized (see Owocki & Zank 1991 for a related discussion). Near the critical point $x = r - R_s$, equation (36) can be extended to include a finite viscosity μ, so that

$$\mu \frac{d^2\eta}{dx^2} = \eta \frac{d\eta}{dx} - a\eta - bx$$

(Owocki & Zank 1991, their eq. [8]). Expanding the right-hand side in the vicinity of the equilibrium solutions $\eta = \eta_0 + y$, we obtain

$$\mu \frac{d^2 y}{dx^2} = \pm \sqrt{a^2 + 4by} , \tag{37}$$

where positive and negative values correspond to those solutions near the corresponding separatrix. One can see that, in general, for $x > 0$, solutions near one of the separatrices are unstable, while all stable solutions are attracted to the second separatrix. Thus, only solutions corresponding to the lower separatrix for $r > R_s$ are meaningful in the case of vanishing

viscosity. On the other hand, all solutions with realistic conditions at $r = 1$ are attracted to the other separatrix at $r < R_s$. This suggests that the sonic transition must be a weak discontinuity in the case of vanishing viscosity.

It is interesting to note that a strong discontinuity, i.e., a shock transition, in the loaded solar wind also has finite jumps in the derivatives. We might then view the termination shock as being a surface of strong discontinuity with an attached weak discontinuity. At the sonic point, the strong discontinuity vanishes, leaving only the weak discontinuity. No stationary discontinuities are possible in the subsonic flow, since $u < c$.

4. SHOCK TRANSITION

In an earlier study of cometary shocks (Galeev & Khabibrakhmanov 1992), we performed a linear stability analysis of a plasma flow loaded by photoionization. It was found that mass loading of the plasma flow has a stabilizing effect for Mach numbers greater then 2.9, but in the range $1 < M < 2.9$, linear perturbations are amplified when propagating along the corresponding characteristic. Hence, in this velocity regime there is an intrinsic instability in the loaded flow that can lead to the development of a gradient catastrophe and the subsequent formation of a shock.

Now we extend the linear stability analysis to include the effects of both charge exchange and spherical expansion, and we apply the results to the interaction of the solar wind with neutral hydrogen. The first step is to transform the original hyperbolic system into characteristic form. The first equation is obtained by adding the pressure and continuity equations (premultiplied by γ). Thus,

$$\hat{D}_0 S = \frac{\beta N \gamma}{\rho r^2}\left(\frac{\gamma - 1}{2} M^2 - 1\right) - \alpha N u\left[1 - \frac{(\gamma - 1)\gamma}{2} M^2\right] = X_S , \tag{38}$$

where

$$S = \ln\left(\frac{P}{\rho^\gamma}\right), \qquad \hat{D}_0 = \frac{\partial}{\partial t} + u \frac{\partial}{\partial r} .$$

The quantity S propagates along the characteristic defined by the operator $\hat{D}_0$ and is proportional to the entropy of the plasma in the gasdynamic sense.

The remaining two equations are obtained in characteristic form from the momentum equation by adding and subtracting the pressure equation [after premultiplication by $1/(\rho c)$]. Thus, we obtain the equations

$$\hat{D}_\pm u \pm \frac{1}{\rho c} \hat{D}_\pm P \pm \frac{vcu}{r} = -\frac{\beta N u}{\rho r^2}\left(1 \mp \frac{\gamma - 1}{2} M\right) - \alpha N u c\left[M \pm \left(\frac{1}{\gamma} - \frac{\gamma - 1}{2} M^2\right)\right] = Y_\pm , \tag{39}$$

where

$$\hat{D}_+ = \frac{\partial}{\partial t} + (u + c)\frac{\partial}{\partial r}, \qquad \hat{D}_- = \frac{\partial}{\partial t} + (u - c)\frac{\partial}{\partial r}$$

are differential operators along the sound characteristics. The system (38)–(39) describes the propagation of entropy and sound disturbances along the corresponding characteristics, together with the stationary solution.

The formation of a discontinuity in hyperbolic systems can result from a "blowup" of the gradients of the flow parameters and is sometimes referred to as a gradient catastrophe. To describe the process, it is convenient to derive transport equations for the spatial derivatives of the flow parameters. The natural choice for these derivatives is

$$K = S_r , \qquad R = u_r + \frac{1}{\rho c} P_r , \qquad L = u_r - \frac{1}{\rho c} P_r . \tag{40}$$

Equations describing the transport of the parameters K, R, and L along the corresponding characteristics are derived by taking spatial derivatives of the equations in characteristic form.

It is convenient to consider the plasma pressure P as a function of density ρ and entropy S. If $P = f(\rho, S) = \rho^\gamma \exp S$, then

$$c^2 = \left.\frac{\partial f}{\partial \rho}\right|_{S = \text{const}} = f_\rho .$$

From this definition, it follows that

$$dc^2 = f_{\rho\rho}\, d\rho + f_{\rho S}\, dS = \frac{f_{\rho\rho}}{f_\rho} dP + f_\rho\left(\frac{f_S}{f_\rho}\right)_\rho dS = \frac{n_0}{\rho} dP + f_\rho n_1\, dS ,$$

$$d(\rho c) = \frac{n_0 + 2}{2c} dP + \frac{\rho c}{2} n_2\, dS , \tag{41}$$

with

$$n_0 = \rho\left(\frac{f_{\rho\rho}}{f_\rho}\right), \qquad n_1 = \left(\frac{f_S}{f_\rho}\right)_\rho , \qquad n_2 = \rho^2\left(\frac{f_S}{\rho^2 f_\rho}\right)_\rho .$$

For a polytropic gas, we have

$$n_0 = \gamma - 1 , \qquad n_1 = 1/\gamma , \qquad n_2 = -n_1 .$$

We can express the spatial derivatives of all the flow parameters in terms of R, L, and K, thereby obtaining the relations

$$u_r = \frac{1}{2}(R + L) , \qquad P_r = \frac{\rho c}{2}(R - L) , \qquad c_r = \frac{n_0}{4}(R - L) + \frac{cn_1}{2} K ,$$

$$(uc)_r = \frac{n_0 u + 2c}{4} R - \frac{n_0 u - 2c}{4} L + \frac{cun_1}{2} K , \qquad \rho_r = \frac{\rho}{2c}(R - L) - \rho n_1 K ,$$

$$M_r = \left(\frac{u}{c}\right)_r = \frac{1}{c^2}\left(-\frac{n_0 u - 2c}{4} R + \frac{n_0 u + 2c}{4} L - \frac{ucn_1}{2} K\right) .$$

Use of the commutation rule for the operators $\hat{D}_\pm$ and $\hat{D}_r$,

$$\hat{D}_r \hat{D}_\pm = \hat{D}_\pm \hat{D}_r + \hat{D}_r(u \pm c)\hat{D}_r ,$$

yields the transport equation for R in the form

$$\hat{D}_+ R + \hat{D}_r(u + c)R + \hat{D}_r\left(\frac{1}{\rho c}\right)\hat{D}_+ P - \hat{D}_+\left(\frac{1}{\rho c}\right)\hat{D}_r P = \hat{D}_r Y_+ - \hat{D}_r\left(-\frac{vcu}{r}\right) . \tag{42}$$

By means of the relations

$$\hat{D}_r\left(\frac{1}{\rho c}\right)\hat{D}_+ P - \hat{D}_+\left(\frac{1}{\rho c}\right)\hat{D}_r P = \frac{n_2}{2\rho c}(P_r \hat{D}_+ S - S_r \hat{D}_+ P) , \tag{43}$$

$$\hat{D}_\pm S = \hat{D}_0 S \pm cS_r = X_S \pm cK , \tag{44}$$

$$\hat{D}_\pm P = \hat{D}_0 P \pm cP_r = -\rho c^2 u_r - \frac{v}{r}\rho c^2 u + X_P \pm \frac{\rho c^2}{2}(R - L) , \tag{45}$$

we can hence obtain the transport equations,

$$\hat{D}_0 K = -\tfrac{1}{2}(R + L)K + \hat{D}_r Y_0 , \tag{46}$$

$$\hat{D}_+ R + \frac{n_0 + 2}{4} R^2 + \left[-\frac{n_0 - 2}{4} L + \frac{2n_1 + n_2}{4} cK + \frac{v}{4r}(2c + n_0 u)\right]R$$

$$+ \frac{n_2}{4} cLK + \frac{v}{2r}(n_1 + n_2)cuK - \frac{v}{4r}(n_0 u - 2c)L - \frac{v}{r^2} cu = -\frac{n_2}{4}(R - L)X_S + \frac{n_2}{4} KX_P + \hat{D}_r Y_+ , \tag{47}$$

$$\hat{D}_- L + \frac{n_0 + 2}{4} L^2 + \left[-\frac{n_0 - 2}{4} R - \frac{2n_1 + n_2}{4} cK + \frac{v}{4r}(n_0 u - 2c)\right]L$$

$$- \frac{n_2}{4} cRK + \frac{v}{2r}(n_1 + n_2)cuK + \frac{v}{4r}(n_0 u + 2c)R - \frac{v}{r^2} cu = -\frac{n_2}{4}(R - L)X_S + \frac{n_2}{4} KX_P + \hat{D}_r Y_- . \tag{48}$$

In the absence of loading, and for an isentropic gas ($K = 0$), we can write the solution for R in the form

$$R = R_0\left(\frac{c^2\rho}{c_0^2\rho_0}\right)^\xi \left[1 + \frac{\gamma + 1}{4\gamma} R_0 \int_{0(C_+)}^{t}\left(\frac{c^2\rho}{c_0^2\rho_0}\right)^\xi dt\right]^{-1} , \tag{49}$$

where

$$\xi = (3 - \gamma)/4\gamma .$$

A similar expression holds for L, if we replace R by L and integrate along the C_- characteristic.

If $R_0 < 0$, the solution diverges in a finite time. This is a common property of hyperbolic systems.

For stationary solutions, we have

$$R = \frac{Y_+ - vcu/r}{u + c} , \qquad L = \frac{Y_- + vuc/r}{u - c} , \qquad K = \frac{X_S}{u} . \tag{50}$$

R changes sign at the point at which the corresponding source term $Y_+ - vcu/r$ is zero; for photoionization, this occurs when $M = 2/(\gamma - 1)$.

We consider linear perturbations in R, L, and K. The transport equations are very convenient for this purpose, as perturbations in L and K are small compared to perturbations in R along the C_+ characteristic. Linearization of the transport

equation for R then gives

$$\frac{1}{\delta R} D_+ \delta R = \frac{\nu c}{r} F_\nu^+(M) + \alpha N c F_\alpha^+(M) + \frac{\beta N}{\rho r^2} F_\beta^+(M) . \tag{51}$$

Similarly, perturbations of L along the C_- characteristic are much greater than those of R and K, and we can linearize easily the transport equation for L to obtain

$$\frac{1}{\delta L} D_- \delta L = \frac{\nu c}{r} F_\nu^-(M) + \alpha c N F_\alpha^-(M) + \frac{\beta N}{\rho r^2} F_\beta^-(M) . \tag{52}$$

The functions F_ν, F_α, and F_β introduced in equations (51)–(52) relate respectively to spherical expansion, charge exchange, and photoionization, and they depend only on the Mach number M; they can be expressed as

$$F_\nu^\pm = -\frac{1}{4(M^2-1)} [(\gamma-1)M^3 \mp 3(\gamma-1)M^2 + 6M \mp 2] , \tag{53}$$

$$F_\alpha^\pm = -\frac{1}{8(M^2-1)} \left[(\gamma-2)(\gamma-1)M^4(M \pm 3) - (2\gamma^2+3\gamma-3)M^3 \pm \left(11\gamma - 13 + \frac{4}{\gamma}\right)M^2 - 2\left(4-\frac{5}{\gamma}\right)M \mp \frac{2}{\gamma}\right] , \tag{54}$$

$$F_\beta^\pm = -\frac{1}{8M(M^2-1)} [\gamma(\gamma-1)M^5 \pm \gamma(3\gamma-7)M^4 - (2\gamma^2+5\gamma-1)M^3 \pm 3(3\gamma-1)M^2 - 6M \pm 2] . \tag{55}$$

We plotted the functions $F_\nu^\pm$, $F_\beta^\pm$, and $F_\alpha^\pm$ for two cases, $\gamma = 2$ and $\gamma = 5/3$, shown in Figure 2. For disturbances propagating along the C_+ characteristic, we see that the spherical expansion term F_ν^+ has a stabilizing effect in the supersonic region of the flow, $M > 1$. For the photoionization term F_β^+, there is a critical Mach number, $M \approx 3$, in the case of $\gamma = 2$, and $M \approx 5$, in the case of $\gamma = 5/3$, so that the stabilizing effect for larger Mach numbers changes into a destabilizing influence at smaller Mach numbers. We observe that charge exchange has a destabilizing effect throughout the supersonic region $M > 1$.

Similar qualitative behavior is observed for the disturbances propagating along the C_- characteristic, but F_β^- changes sign at $M \approx 3$ in both cases.

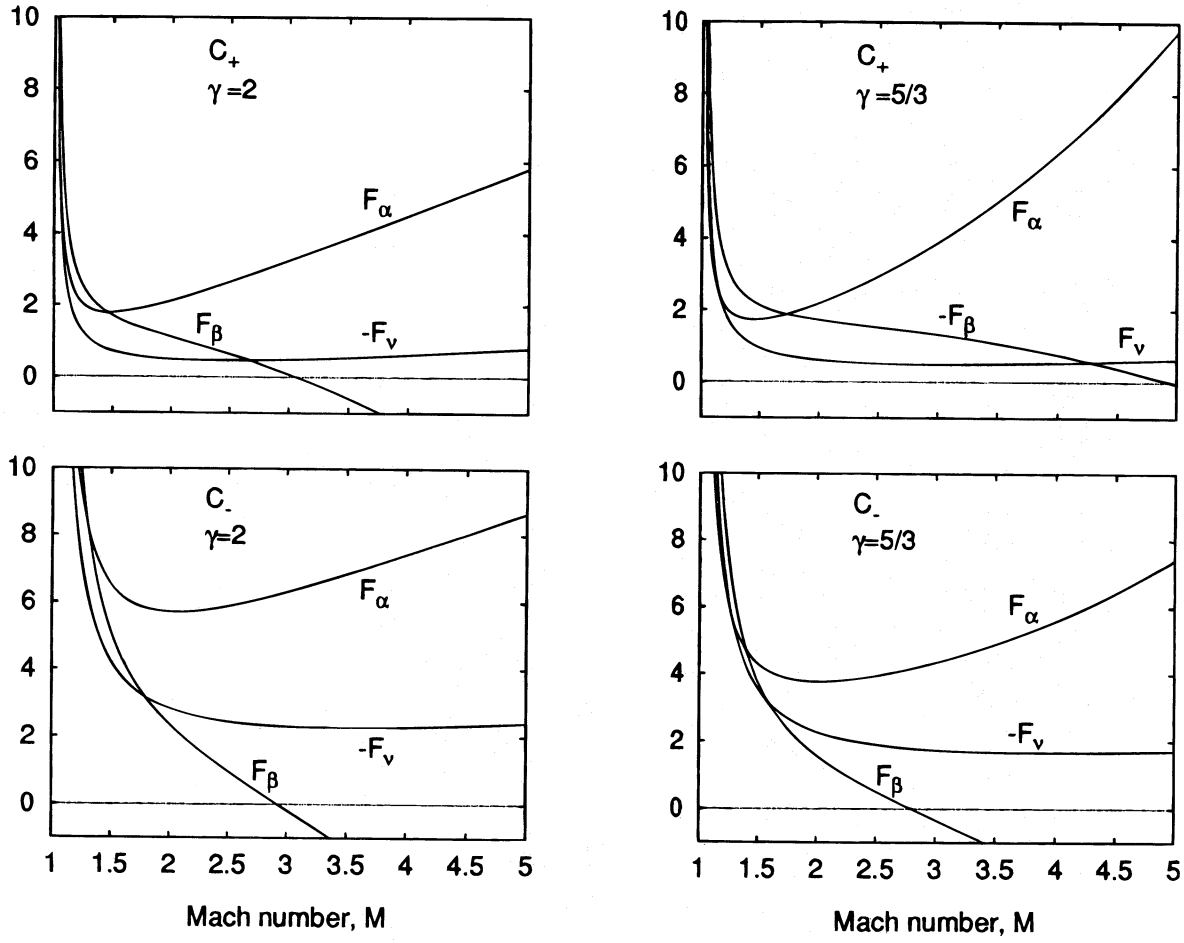

FIG. 2.—Dependence of the functions F_ν, F_α, and F_β on the Mach number M for $\gamma = 2$ (*left*) and $\gamma = 5/3$ (*right*), for disturbances propagating along the C_+ characteristic (*top*) and C_- characteristic (*bottom*).

As a result of the r^{-1} dependence, the expansion term in equations (51) and (52) dominates at small distances, but there is a critical point in the flow, at M_{cr}, at which charge exchange becomes competitive and destabilizes the flow at larger distances and smaller Mach numbers. This situation is clear from Figure 3, in which a Mach number profile for the stationary solution is shown together with the marginal stability curve defined by

$$r = -\frac{v}{\alpha N}\frac{F_v^{\pm}}{F_\alpha^{\pm}}, \tag{56}$$

for the cases $\gamma = 2$ and $\gamma = 5/3$. To the right of the marginal stability curve, the flow is unstable. For the $\gamma = 2$ case, we see that the critical Mach number $M_{cr}^{+} = 3$ is reached at $r_{cr}^{+} = 50$ AU for the C_+ characteristic, and the flow stabilizes again for $M < 1.8$ in the region $r > 140$ AU. Disturbances propagating along the C_- characteristic are stable for $M > 1.8$. A remarkable feature is that for the region in which the Mach number $M < 3$, the marginal stability curve for C_+ lies very close to the Mach number profile, meaning that the destabilizing effect of charge exchange is compensated for largely by the effect of spherical expansion. In that case, destabilization associated with photoionization at $M < 3$ could be important. For $\gamma = 5/3$,

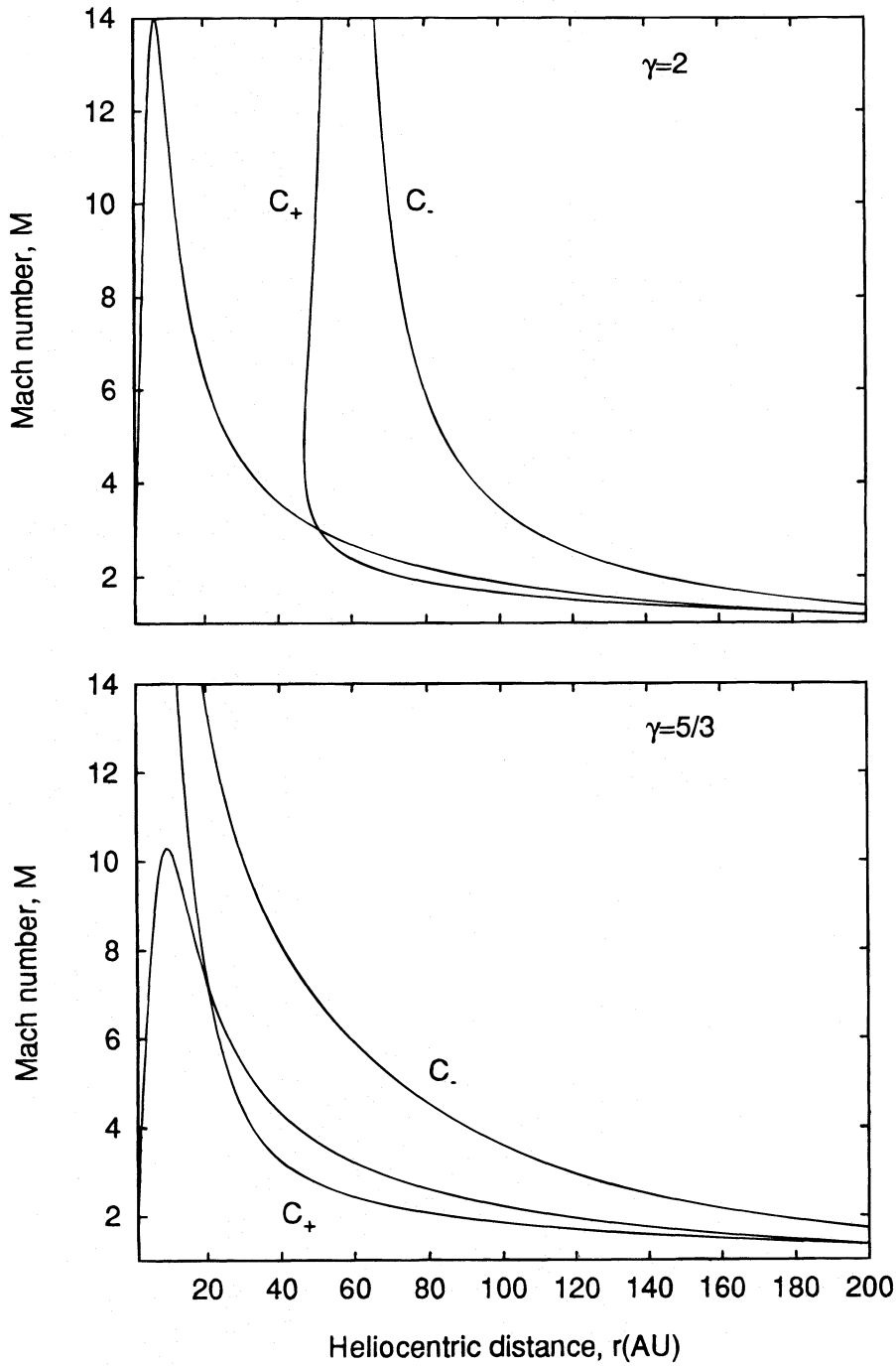

FIG. 3.—Marginal stability curves for disturbances propagating along the C_+ and C_- characteristics, together with the Mach number profile corresponding to $M = 2$ at $r = 1$ AU, for $\gamma = 2$ (*top*) and $\gamma = 5/3$ (*bottom*).

similar qualitative behavior is found. Disturbances propagating along the C_+ characteristic are destabilized at Mach numbers in the range $7 < M < 1.8$, which corresponds to the region 25 AU $< r <$ 170 AU. Thus, we might conclude that a termination shock may form as a result of a gradient catastrophe in the quantity $R = u_r + P_r/(\rho c)$ along the C_+ characteristic in the region $r > 25$ AU for $\gamma = 5/3$, and in the region $r > 50$ AU for $\gamma = 2$. A finite photoionization rate tends to increase the critical Mach number toward the value $M = 3$ for $\gamma = 2$, and toward $M = 5$ for $\gamma = 5/3$. Thus, the flow is even more unstable for smaller Mach numbers, and so these numbers give a most probable Mach number for the discontinuity.

Recently, Pauls et al. (1995) developed a two-dimensional hydrodynamic model of the solar wind–LISM interaction that is fully self-consistent in the sense that both the neutral and plasma components are determined simultaneously. The model has since been extended to solve the Boltzmann equation for the interstellar neutrals directly. By way of example, we have plotted in Figure 4 a purely gasdynamic calculation (i.e., all effects of neutrals, charge exchange, and photoionization are neglected) for LISM parameters that correspond to a supersonic interstellar wind. In Figure 5, the corresponding solution obtained from a kinetic code (Zank et al. 1995), which now includes the neutrals, is shown. It is clear that the location of the termination shock (and heliopause and bow shock) is dramatically different for the two cases. Plotted in Figure 6 is the solar wind Mach number along the stagnation line out to the termination shock. In the purely gasdynamic example, the Mach number of the solar wind becomes very large before the wind terminates at a very strong shock, with a compression ratio close to the maximum possible value of 4. By contrast, the Mach number for the loaded solar wind diminishes with radial distance, and the termination shock, located at about 70 AU, is significantly weaker. It is of interest to observe that the Mach number of the termination shock for the loaded wind is $M \simeq 4.5$, in approximate agreement with the critical Mach number $M = 5$ for $\gamma = 5/3$. As the simulations were performed with the specific heat ratio $\gamma = 5/3$, which corresponds to a shell distribution of

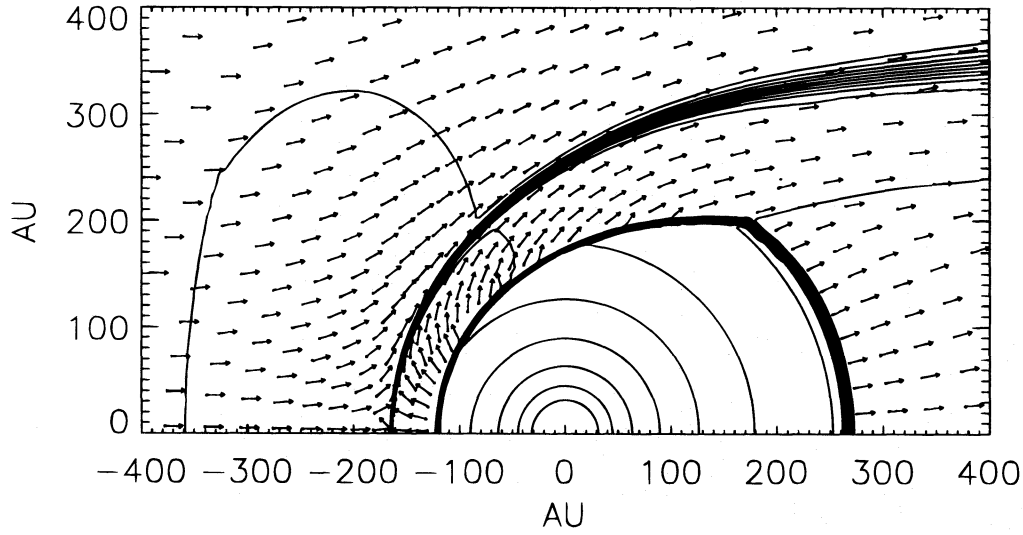

FIG. 4.—Normalized density contours ($\rho_{H^+}/\rho_{H\infty}$) and the normalized flow speed vectors of the protons in the case without charge exchange. Solid lines denote densities greater than or equal to $\rho_{H\infty}$, while dotted lines denote densities less than $\rho_{H\infty}$.

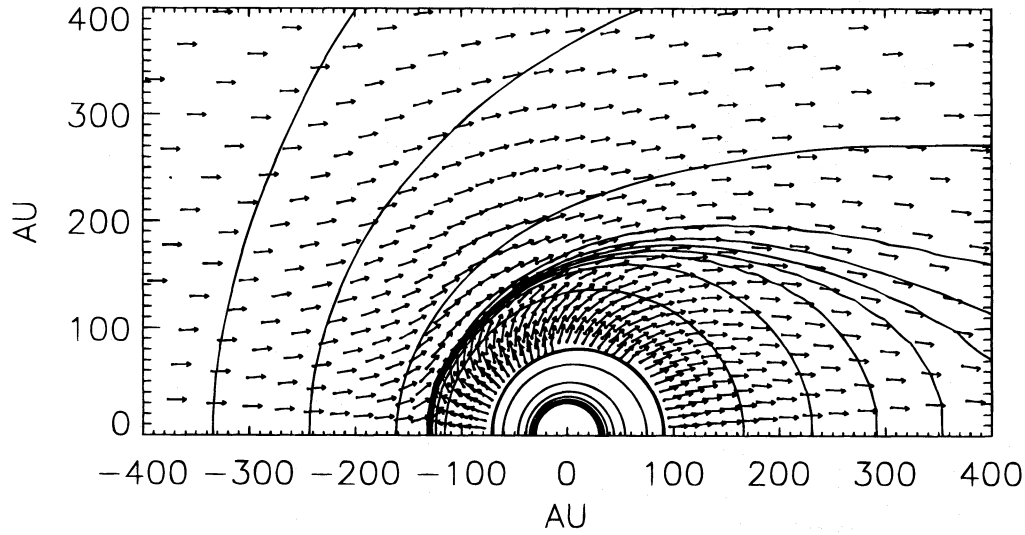

FIG. 5.—Same as Fig. 4, except that charge exchange is included self-consistently here

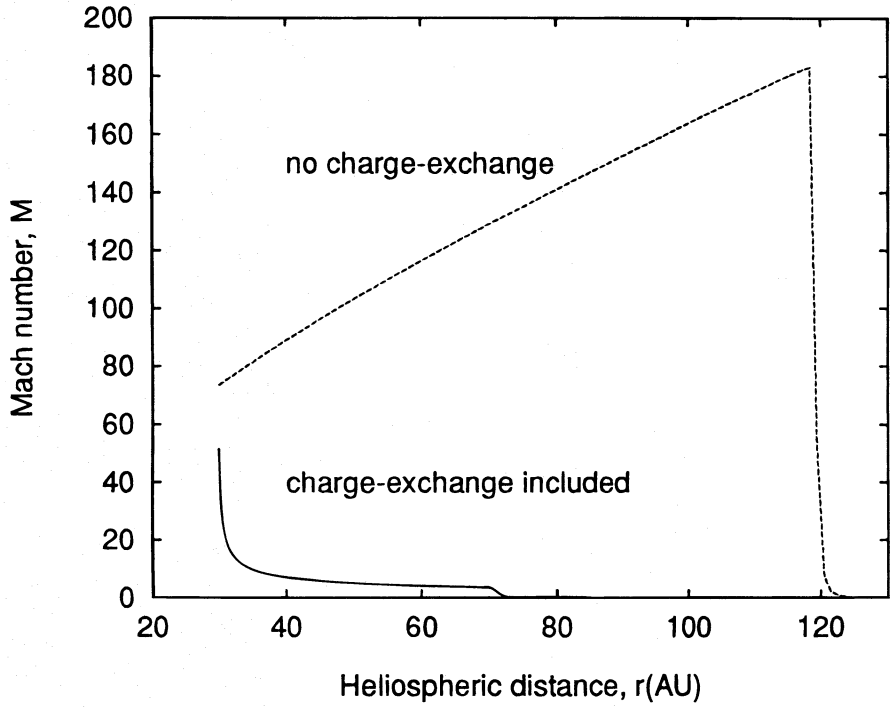

FIG. 6.—Mach number profiles with and without charge exchange

pickup ions, this indicates that self-consistent simulations do reflect the unstable nature of the loaded plasma flow at low Mach numbers. What is different, however, is that such a Mach number occurs only at a heliocentric distance of about 70 AU, and not at the 35 AU obtained above. The difference results from our using a non–self-consistent description of the neutral interaction with the solar wind, unlike in the kinetic simulation model. The reason for this shift is clear from the self-consistent neutral particle profile in Figure 7 obtained in numerical simulations. There is a remarkable deviation from the simple exponential law described by the zero-order solution of equation (24). This indicates that the modifications of the neutral density profile due to the finite right-hand side of equation (24) are important in understanding the physics of outer heliosphere.

The region 120 AU $< r <$ 220 AU is the interface between the two colliding plasmas, the solar wind plasma and the LISM, and it is characterized by significant variations in all the parameters describing the neutral particles. There is an accumulation of neutral particles, leading to an increase in particle density by a factor of 2, accompanied by heating and a slowing down of their flow. These effects are attributed to repetitive charge exchange of the neutral particles. Most interestingly, on the inner side of the interface region, the neutral particle density is halved with respect to the neutral density at large distances. Thus, the parameters α and β in our model should be decreased by a factor of 2 to take this effect into account. It is clear that the main effect of this is to double the characteristic spatial dimensions at large distances, so that the Mach number $M = 4.5$ will shift from 35 AU to 70 AU.

We should note here that in the outer heliosphere, owing to the spiral nature of the magnetic field, a quasi-perpendicular geometry is expected to prevail. In this case, pickup ions have a ring-type distribution in velocity space, and their specific heat ratio should be close to 2. We do not have numerical simulation results for this case at present, and so we cannot estimate interface effects, but our analytical model predicts the Mach number of the termination shock to be $M = 3$ at a distance $r = 50$ AU, for $N_\infty = 0.1$ cm^{-3}. Some interface effect similar to that discussed above might increase the distance to the termination shock, but the strength of the termination shock, expressed quantitatively by its Mach number M, is invariant. Thus, the one-dimensional model presented here and the numerical simulations illustrate that the outer heliospheric structure and properties may well be determined by the properties of the neutral interstellar hydrogen gas component.

5. CONCLUSIONS

A simple gasdynamic system describing the interaction of the solar wind flow with neutral hydrogen via charge exchange and photoionization has been formulated using a microscopic description. Our analysis clarifies the origins of the hydrodynamic models developed originally by Wallis (1971) and Holzer (1972). We have considered the system for the stationary case, and we have discussed the stability properties of the solutions. We have shown that charge exchange has a destabilizing effect on the plasma flow in the supersonic region as a whole. Although spherical expansion can stabilize the flow at high Mach numbers, its effect diminishes in favor of charge exchange beyond a critical Mach number. We deduce from this that loading of the plasma flow at high Mach numbers results in a smoothing of small perturbations, so that the resulting plasma flow should be relatively quiescent. At lower Mach numbers, however, small perturbations propagating downstream are amplified. Under these circumstances, we expect the plasma flow to become more "turbulent" far from the Sun, with the possibility of a gradient catastrophe developing, and the subsequent formation of the termination shock. Fully self-consistent multidimen-

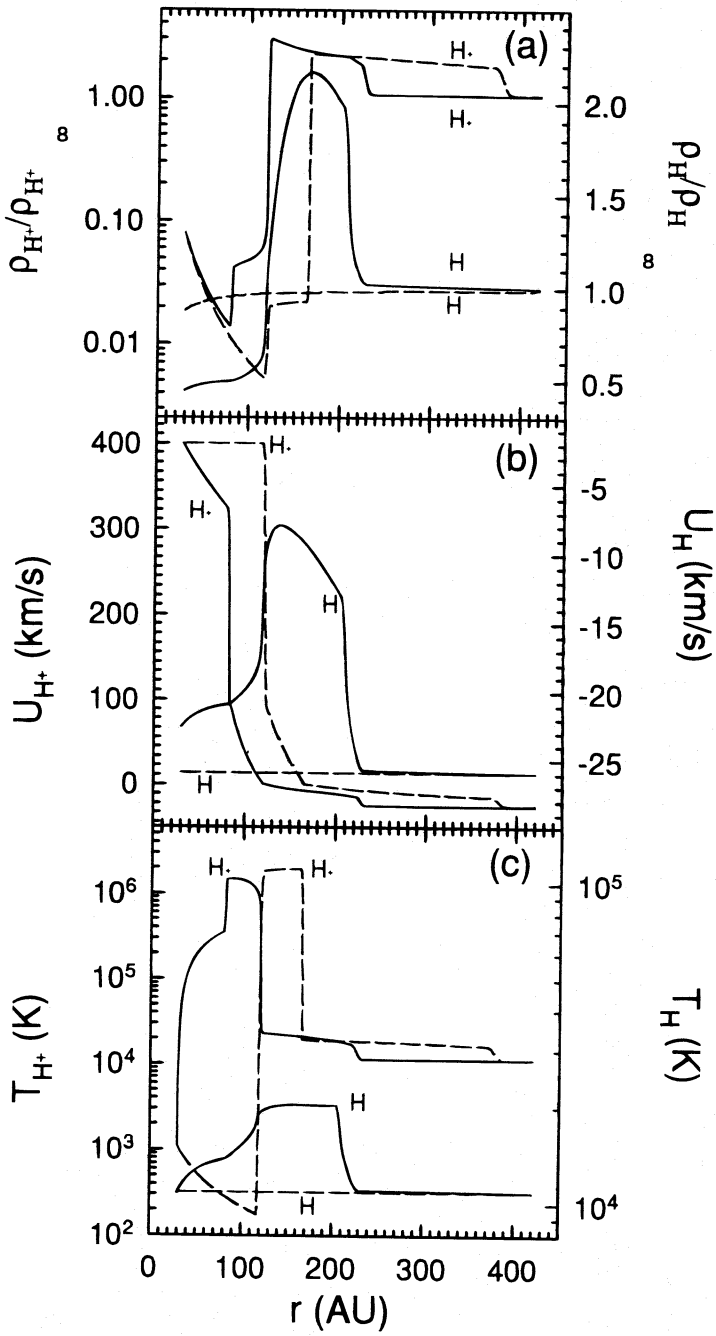

FIG. 7.—Numerical solutions for the plasma and neutral hydrogen density, bulk speed, and temperature profiles according to calculations by Pauls et al. (1995). Dashed lines represent the case of direct solar-interstellar wind interaction. Solid lines represent the case of inclusion of charge exchange between the plasma and neutral components.

sional simulations appear to support this conclusion, with the formation of the termination shock at a Mach number $M = 4.5$ at $r = 70$ AU, for a specific heat ratio of $\gamma = 5/3$ for the pickup ions. If, however, quasi-perpendicular geometry prevails in the distant heliosphere, so that $\gamma = 2$, the termination shock should be even weaker, with $M = 3$ at a distance of $r = 50$ AU, corresponding to an interstellar hydrogen density $N_{\infty} = 0.1\ \mathrm{cm}^{-3}$.

In summary, we find that the properties of the interstellar neutral gas play a critical role in determining the nature and characteristics of the plasma structure in the outer heliosphere.

This work is supported by the Natural Sciences and Engineering Research Council of Canada under grant A-0621, and by funds from the Dean of Science, Memorial University of Newfoundland. G. P. Z. and H. L. P. acknowledge partial support from NASA grants NAGW-3450, NAGW-2076 and an NSF Young Investigator Award ATM 93-57861. Computations were performed on the Cray Y-MP at the San Diego Supercomputer Center.

REFERENCES

Baranov, V. B. 1990, Space Sci. Rev., 52, 121
Galeev, A. A. 1991, in Comets in the Post-Halley Era, Vol. 2, ed. R. L. Newburn, Jr., M. L. Neugebauer, & J. Rahe (Norwell, MA: Kluwer), 1145
Galeev, A. A., & Khabibrakhmanov, I. K. 1992, in Plasma Environments of Non-Magnetic Planets, COSPAR Colloq. Vol. 4, ed. T. I. Gombosi (Oxford: Pergamon), 21
Holzer, T. E. 1972, J. Geophys. Res., 77, 5407
———. 1989, ARA&A, 27, 199
Holzer, T. E., & Banks, P. M. 1969, Planet. Space Sci., 17, 1074
Khabibrakhmanov, I. K., Galinsky, V. L., & Verheest, F. 1992, Phys. Fluids B, 4, 2538
Kulsrud, R. M. 1983, Basic Plasma Physics I, ed. A. A. Galeev & R. N. Sudan (New York: North-Holland), 115
Lallement, R., Bertaux, J.-L., & Clarke, J. T. 1993, Science, 260, 1095
Landau, L. D., & Lifshitz, E. M. 1987, Fluid Mechanics (2d ed.; Oxford: Pergamon)
Owocki, S., & Zank, G. P. 1991, ApJ, 368, 491
Parker, E. 1958, ApJ, 128, 664
Pauls, H. L., Zank, G. P., & Williams, L. L. 1995, J. Geophys. Res., 100, 21595
Wallis, M. 1971, Nature, 233, 23
Zank, G. P., Pauls, H. L., Williams, L. L., & Hall, D. 1995, J. Geophys. Res., in press